Experimental Loss Separation of Mega-hertz Inverter for WPT System using Calorimetric Power Loss Measurement

Masamichi Yamaguchi
Dept. of Science of Technology Innovation
Nagaoka University of Technology
Nagaoka, Niigata, Japan
m_yamaguchi@stn.nagaokaut.ac.jp

Keisuke Kusaka
Dept. of Electrical, Electronics and Information Engineering
Nagaoka University of Technology
Nagaoka, Niigata, Japan
kusaka@vos.nagaokaut.ac.jp

Jun-ichi Itoh
Dept. of Electrical, Electronics and Information Engineering
Nagaoka University of Technology
Nagaoka, Niigata, Japan
itoh@vos.nagaokaut.ac.jp

***Abstract*— This paper discusses a power loss, which occurs in a load-resonant inverter operating at megahertz for wireless power transfer (WPT) systems. A calorimetric method is applied to measure the power losses in the mega-hertz operation accurately. The loss is measured using a single chamber with temperature control of the internal chamber using a Peltier device. The loss can be measured within 10% error when the loss is less than 23 W with a prototype chamber in experiment. A drive circuit loss, conduction loss of GaN devices, and PCB pattern loss are measured using the measurement site. Moreover, the total loss of the inverter with 6.78-MHz operation is measured under the zero voltage switching (ZVS) condition. The losses on the inverter are separated by a combination of each measurement result. As a result, the loss, which is related to the mega-hertz operation under the ZVS condition, is 9.9 W when the output power is 417 W at 6.78-MHz operation.**

Keywords*— high-frequency inverter, calorimetric power loss measurement

I. INTRODUCTION

In recent years, battery chargers for electric vehicles (EVs) have been installed rapidly by increasing the interest in EVs. Notably, wireless power transfer (WPT) systems for battery chargers have been actively studied from the safety and convenience perspective in this decade. Especially, rapid charging is required for EVs to reduce the charging time because the charger using the WPT system takes a long time to charge the onboard batteries. Thus, increasing the power density of the WPT system is urgent.

A transmission frequency of 85 kHz is used in the standardization of WPT systems. However, the 85 kHz system is bulky and heavy because the WPT system has a ferrite in transmission coils. A heavy system on the vehicle directly causes an increase in power consumption during the running. Employing mega-hertz order switching frequency is one of the solutions to achieve high power density and a light system. Thus, the mega-hertz operation in a WPT system has been actively studied [1-2].

An inverter circuit for the mega-hertz operation requires nano-second order switching. GaN-transistors, which can switch in a few nano-second, are used for these high-frequency WPT systems. A surface-mounted device (SMD) package is commonly adopted to the GaN-transistor because the SMD allows decreasing a parasitic inductance on the devices. Although, SMD has a small heat spreader because the package size is small. Thus, the design of heat dissipation of devices is a critical issue for mega-hertz operation.

The accurate calculation of thermal resistance and estimation of the loss of devices is essential for thermal design. However, accurate measurement of devices loss based on the voltage and current is difficult in mega-hertz operation because the difficulty of accurate measurement with mega-hertz voltage and current is still high. It prevents an accurate thermal design and decreases power density.

A loss measurement based on the thermal measurement has been conducted in recent studies[3-18]. Ref. 3 shows the loss measurement of the full-bridge converter, which employs a GaN-transistor. The calculation and measurement result shows good agreement, although the converter is operated at 160 kHz. Ref. 4 investigates a calorimetric method for loss measurement of the SiC-MOSFET. However, the switching frequencies higher than 1 MHz have not been investigated.

In this paper, the breakdown of power loss caused by the mega-hertz resonant inverter is experimentally analyzed with the calorimetric method. The calorimetric method is based on the thermal measurement without sensing voltage and current of the main circuit. Thus, the loss can be measure accurately even though the circuit as the device under test (DUT) is operated in megahertz. The losses are experimentally separated into a drive circuit loss, a conduction loss of the GaN-devices, and a conduction loss of a PCB pattern. As a result, the loss, which is related to the mega-hertz operation under the ZVS condition, is clarified by a combination of the result of each measurement.

II. CALORIMETRIC LOSS MEASUREMENT

A. Load-resonant Inverter as DUT

Figure 1 shows the circuit configuration of the mega-hertz resonant inverter as a DUT in loss measurement. The GaN-transistors (PGA26E07BA: 600 V, 26 A, Panasonic) are used for the mega-hertz switching (6.78MHz). The resonant load is connected to the output side as the primary side of a WPT system. The ZVS should be achieved to reduce the switching loss on the transistor. Thus, the resonant frequency of the resonant load is selected to the 6.34 MHz because the phase of the load current should be lag to achieve the ZVS condition.

Figure 2 shows the voltage waveforms of the inverter output at 6.78 MHz. The DC link voltage is 150 V. The ZVS condition is achieved at the output voltage. The RMS value of the voltage at load resistor v_{load} is 91.4 V. The load resistance

978-1-6654-3448-5/21/$31.00 ©2021 IEEE

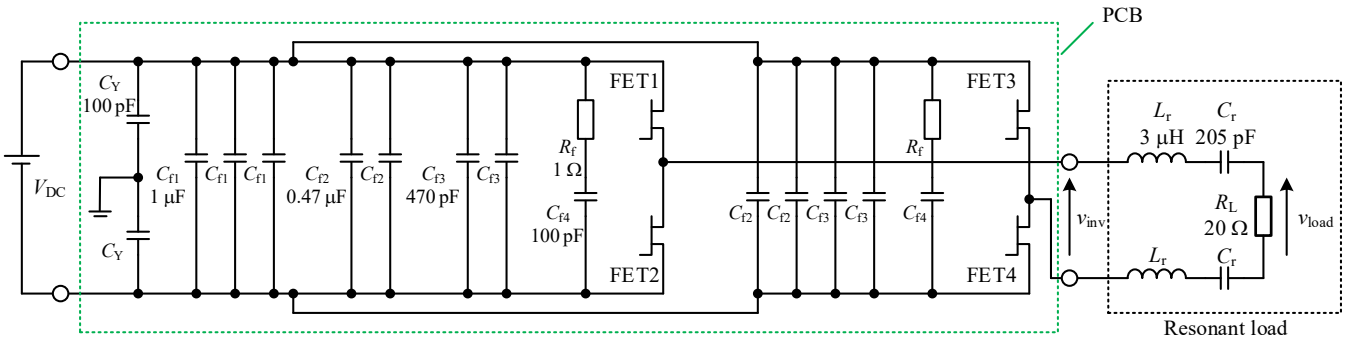

Fig. 1. Mega-hertz resonant inverter.

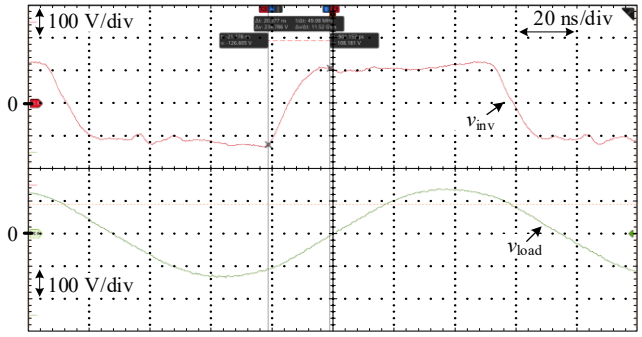

Fig. 2. Voltage of inverter output and load resistor.

is 20 Ω. Thus the calculated output current is 4.6 A in this operation. Figure 3 (a) shows a thermal picture of the inverter circuit with 75 W output, and figure 3(b) shows the outlook of the circuit. The main thermal sources are GaN-transistors in the main circuit and isolated DC/DC converter ICs in a gate drive circuit.

B. Calorimetric Method with Single Chamber

The calorimetric method is used to measure the power loss based on a thermal measurement of the DUT. Figure 4 shows a configuration of the measurement system applying a calorimetric method with a single chamber[5]. The DUT is operated in the chamber, which has a Peltier device as a heat exchanger to control an internal temperature constantly. The power loss of the DUT can be calculated by the endotherm of the Peltier device when the internal temperature is kept constant. The endotherm of the Peltier device is expressed by

$$P_{\text{loss}} = S_p T_c I_p - \frac{T_h - T_c}{R_p} - \frac{1}{2} r_p I_p^{\,2} \quad \text{..... (1)},$$

where S_p is the Seebeck coefficient, T_c is the temperature of the cold side, T_h is the temperature of the hot side, R_p is the thermal resistance, r_p is electric resistance, I_p is the current of the Peltier device. The chamber has a fan motor to make an air circulation in the chamber. Thus, the loss value of the DUT is expressed by

$$P_{\text{loss}} = S_p T_c I_p - \frac{T_h - T_c}{R_p} - \frac{1}{2} r_p I_p^{\,2} - P_{\text{FC}} \quad \text{..... (2)},$$

where P_{FC} is the power loss of the internal fan motor.

Figure 5 shows the PI controller for the internal temperature control. In this investigation, the internal temperature is controlled to the same as the ambient temperature because the thermal flow, which through polystyrene wall, cannot be ignored if the temperature difference is large.

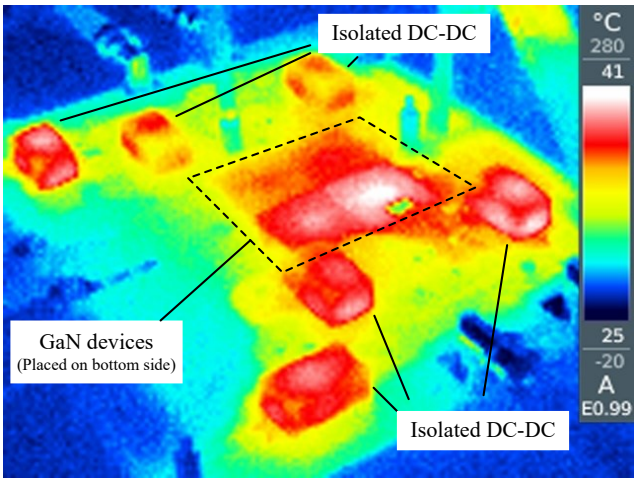

(a) Heat distribution on circuit.

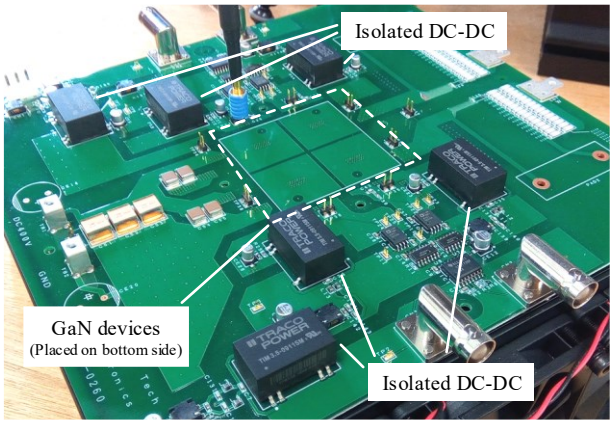

(b) Outlook of circuit.

Fig. 3. Load-resonant inverter as DUT.

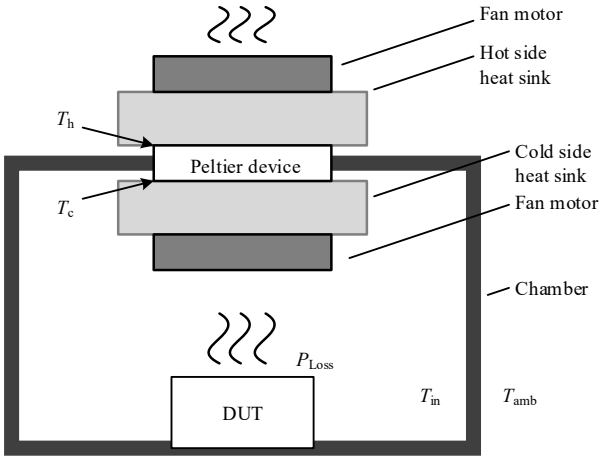

Fig. 4. Calorimetric power loss measurement with single chamber.

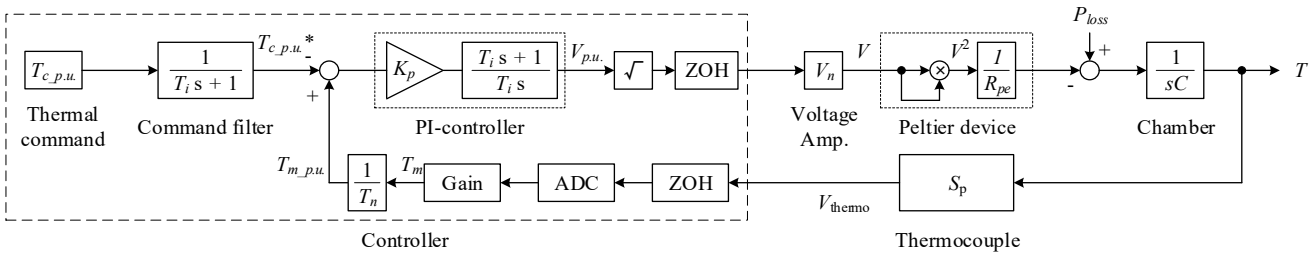

Fig. 5. Thermal control system for calorimetric power loss measurement.

Figure 6 shows a prototype of the measurement site based on the calorimetric method with the single chamber. The chamber is made from expanded polystyrene with a thickness of 20 mm. The mega-hertz resonant inverter is operated in this chamber as the DUT. The resonant load is placed outside of the chamber and connected to the inverter circuit by cable. Table 1 shows the parameter of the prototype of the measurement site.

The accuracy of the measurement site with the temperature control is validated using a known resistor with DC-current on the DUT. The accuracy of the loss measurement is 3.6% at 5.1 W and 7.3% at 23.0 W. Thus, the accuracy of the measurement site is sufficient to measure the circuit losses.

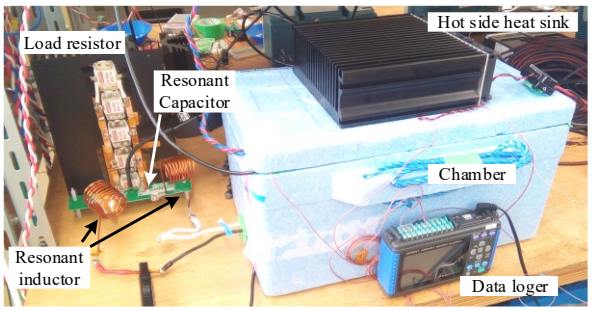

Fig. 6. Loss measurement site.

Table 1. Parameter of measurement site.

Peltier device		
Thermopower	S_p	0.0564 V/K
Thermal resistance of Peltier device	R_p	1.58 K/W
Resistance of Peltier device	r_p	3 Ω
PI controller		
Respons frequency	f_r	0.002 Hz
Attenuation coefficient	ζ	0.5
Thermal capacitance in Chamber	C	31.5 J/K

III. Experimental Loss Breakdown

The loss of a device should be clarified although the total loss value in the chamber can be measured by the calorimetric method. This is because the loss of the device is the most important point in the thermal design. Thus, the loss of other components, drive circuit, and the PCB pattern, are separated by a combination of some measurements result.

Moreover, the loss on the transistor consists of the conduction loss and the switching loss. Especially, the switching loss, which is related to the switching frequency, should be revealed in the mega-hertz operation. Thus, the loss measurement flow in order to separate the cause of losses is as follows.

A. Drive circuit loss

First, a drive circuit loss is measured without applying DC-link voltage. The drive circuit loss is caused by a gate current, which conducts from the drive circuit to the input capacitance of transistors C_{iss} when transistors switch. The drive loss increases with the switching frequency. Thus, the drive loss is measured from DC to 6.78 MHz in 1.695 MHz increments.

The drive loss changes with DC-link voltage V_{DC} because the C_{iss} changes with the v_{ds}. However, the variation of the C_{iss} is relatively small (C_{iss} = 550 pF at v_{ds} = 0 V, C_{iss} = 405 pF at v_{ds} = 400 V). Thus, the measured loss value at mega-hertz operation without DC-link voltage is considered as the drive loss.

Figure 7 shows the measurement result of the drive circuit loss based on (1). The drive circuit loss is 4.6 W at 6.78-MHz operation, and the loss at 0 Hz (DC) is 3.5 W. The drive circuit loss consists of a proportional term to the switching frequency and constant term, which is dominant in the drive circuit loss. The main cause of the constant loss is considered as the power consumption of isolated DC/DC ICs on the drive circuit.

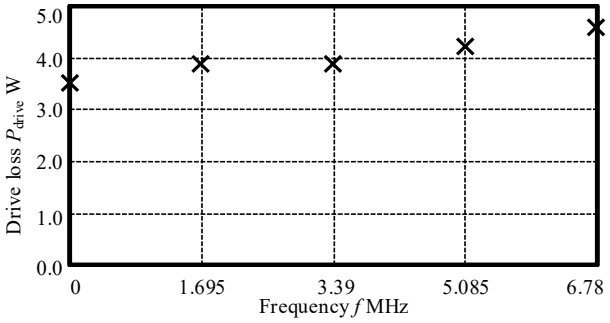

Fig. 7. Drive circuit loss of inverter.

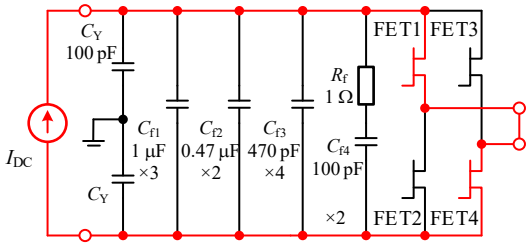

Fig. 8. Circuit connection at conduction loss measurement.

B. *Conduction loss of GaN-transistor*

Second, a conduction loss of GaN-transistors is measured with DC-current. Figure 8 shows the circuit connection at the conduction loss measurement of the GaN-transistors. The input side of the DC-link is connected to a constant current supply, and the output terminal of the inverter is shorted. DC-current is conducted to two GaN-transistors, which are implemented to an opposite side of each arm in the H-bridge. The DC-current value is selected to be the same as the RMS value in the mega-hertz operation. The current of 1.6 A, 3.2A, and 4.6A are selected as the DC-current value. The measurement result involves the conduction loss of the GaN-transistor and the drive loss, which is measured in the section A. Thus, the drive loss at the DC is subtracted from the measured value to compensate for the conduction loss.

Figure 9 shows the measured conduction losses of GaN-devices with the DC-current. The conduction loss with 1.6 A cannot be measured because the loss value is very small. The theoretical conduction loss is about 0.3 W based on an on-resistance of the GaN-transistor at 1.6 A (at junction temperature T_j = 25°C). The measured loss at 3.2 A shows good agreement with the theoretical loss at T_j = 25°C.

On the contrary, the measured loss at 4.6 A has a difference of about 2.3 W from the theoretical loss at T_j = 25°C. The reason for the loss difference is considered as the difference in junction temperature. The theoretical loss at 4.6 A with T_j = 75°C shows good agreement. Although the difference based on the junction temperature occurs in the measured result, the difference can be ignored in the following consideration because the difference value is relatively small compared to the total loss value.

C. *Conduction loss of PCB pattern*

The conduction loss on a current path is increased by a skin effect in mega-hertz operation. The skin depth δ is expressed as:

$$\delta = \frac{1}{\sqrt{\pi f \mu_0 \sigma_2}} \quad \text{..... (3),}$$

where f is frequency and σ_2 is the conductivity of a material. The skin depth is about 25 μm in 6.78 MHz. The top and the bottom layer have 70 μm thickness in the inverter circuit. Thus, the skin effect should be considered in the measurement of conduction loss of the PCB pattern.

Figure 10 shows the circuit connection at the conduction loss measurement of the PCB pattern. The path of the mega-hertz current, DC-link capacitor and two GaN-transistors, are shorted. The output terminal of the inverter is connected to the mega-hertz current supply. The pattern loss is measured with the mega-hertz current to include the influence of the skin effect. Figure 11(a) shows the thermal picture with a current of 4.6 A, and figure 11(b) shows the circuit photo from the same angle. The pattern, especially near the output terminal, has been heated. This is because the pattern width near the output terminal is narrow due to the limitation of the board layout.

Figure 12(a) shows the conduction losses of the PCB pattern with a current of 3.2 A and 4.6 A. The conduction loss increases as the switching frequency in each current condition.

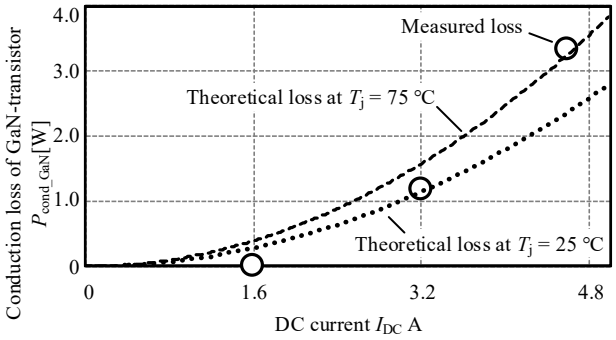

Fig. 9. Conduction loss of GaN-transistors.

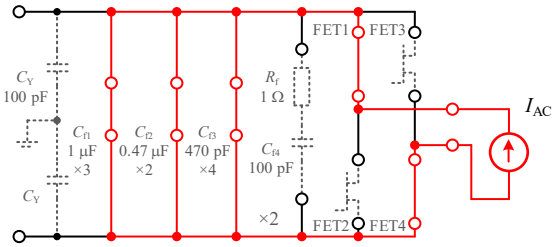

Fig. 10. Circuit connection at loss measurement of PCB pattern.

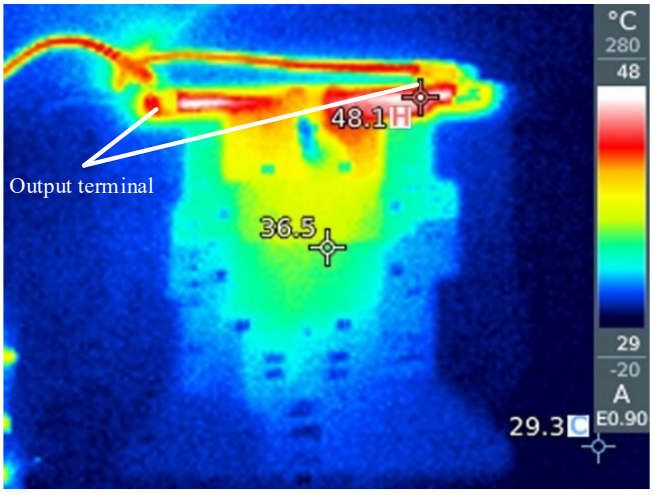

(a) Heat emission from PCB pattern.

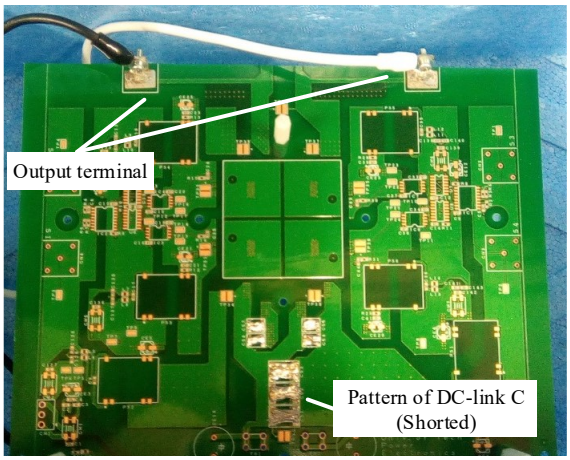

(b) Circuit connection.

Fig. 11. Loss measurement of PCB pattern.

The cause of the loss increment is considered as the influence of the skin effect.

Figure 12(b) shows the conduction loss of the PCB pattern at 6.78MHz. The measured result is approximated to the quadratic equation as

$$P_{\mathrm{PCB}} = 0.224I^2 + 0.552I \quad \text{..... (4).}$$

The quadratic term is considered as the pattern resistance at 6.78 MHz. The proportional term is considered as the increases of R_{PCB} by the heating. The measurement result implies that the PCB pattern should be designed on the viewpoint about parasitic resistance, which is considered of the skin effect, and the heat dissipation of the pattern.

D. Total loss at mega-hertz operation

Finally, a total loss of the inverter at the mega-hertz operation is measured. The RMS value of the output current is 1.6 A, 3.2 A, and 4.6 A when the DC-link voltage is 50 V, 100 V, and 150 V. The output power at load resistor is 417 W when the DC-link voltage is 150 V. The inverter is operated by the ZVS condition at 6.78 MHz. In general, the switching loss is zero under ZVS conditions on switching devices. In this investigation, the drive loss, the conduction loss of the GaN-transistor, and the PCB are subtracted from the total loss in order to clarify the loss, which is related to the switching frequency.

Figure 13 shows the loss measurement result with a 6.78-MHz operation. The total loss is 24.6 W when V_{DC} is 150 V. Then, loss excluding the drive and conduction loss from the total loss is defined as another loss. Another loss is about 9.9-W when V_{DC} is 150 V. Another loss is caused by the mega-hertz operation. The causes of another loss can be considered as the increasing parasitic resistance on the GaN-transistor by the skin effect, and snubber loss in the mega-hertz operation.

IV. Conclusions

This paper investigates a power loss of the load-resonant inverter in the mega-hertz operation. The calorimetric method is applied to measure the loss in mega-hertz operation accurately. The measurement error of the losses achieves within 10% using a single chamber with a Peltier device. The drive loss, the conduction loss of the GaN-transistor, conduction loss of the PCB pattern, and total loss are measured respectively by the calorimetric method. Particularly, the total loss of the inverter with 6.78-MHz operation is measured under the ZVS condition. The losses on the inverter are separated by a combination of each measurement result. Measurement results show that the loss, which is caused by the mega-hertz operation, exists in the load resonant inverter at the mega-hertz operation under the ZVS condition. The consideration of the influence of the junction temperature and loss of the passive components like a snubber circuit are future works.

Acknowledgment

This work was supported by Council for Science, Technology and Innovation (CSTI), Cross-ministerial Strategic Innovation Promotion Program (SIP), “Energy systems of an Internet of Energy (IoE) society” (Funding agency: JST).

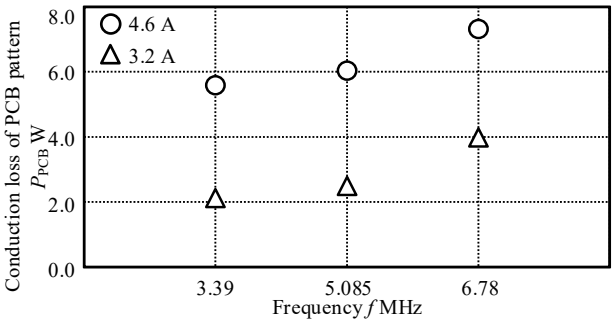

(a) Difference of switching frequency.

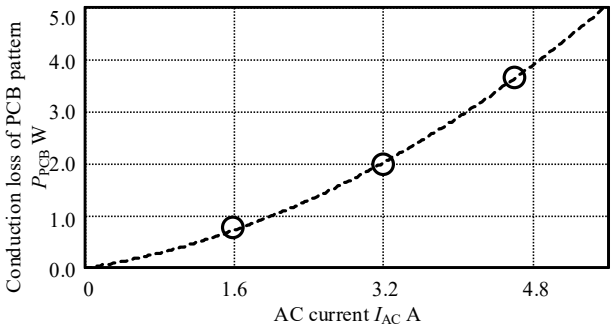

(b) Loss measurement with 6.78 MHz.

Fig. 12. Conduction loss of PCB pattern.

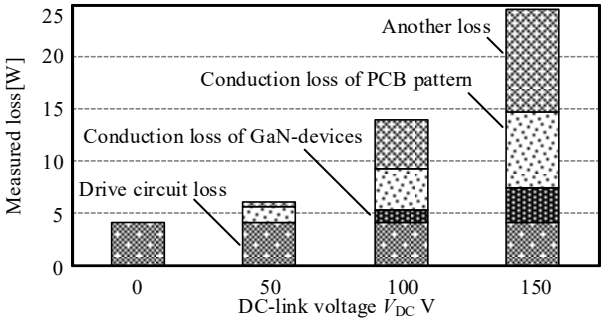

Fig. 13. Total loss of inverter circuit with 6.78 MHz operation.

References

[1] M. Liu, M. Fu, Y. Wang and C. Ma, "Battery Cell Equalization via Megahertz Multiple-Receiver Wireless Power Transfer," in IEEE Transactions on Power Electronics, vol. 33, no. 5, pp. 4135-4144(2018)

[2] L. Jiang and D. Costinett, “A High-Efficiency GaN-Based Single-Stage 6.78 MHz Transmitter for Wireless Power Transfer Applications,” IEEE Transactions on Power Electronics, vol. 34, no. 8, pp. 7677-7692(2019)

[3] W. Meng, F. Zhang, G. Dong, J. Wu and L. Li, "Research on Losses of PCB Parasitic Capacitance for GaN-Based Full Bridge Converters," in IEEE Transactions on Power Electronics, vol. 36, no. 4, pp. 4287-4299, April 2021.

[4] A. Anurag, S. Acharya and S. Bhattacharya, "An Accurate Calorimetric Loss Measurement Method for SiC MOSFETs," in IEEE Journal of Emerging and Selected Topics in Power Electronics, vol. 8, no. 2, pp. 1644-1656, June 2020.

[5] K. Mitsugi, Y. Noge, and M. Deng, “Simple Calorimetric Power Loss Measurement System Using Single Chamber and Peltier Device with Ambient Temperature Tracking Control,” 2020 IEEE Applied Power Electronics Conference and Exposition (APEC), pp. 393-398(2020)

[6] D. Rothmund, D. Bortis and J. W. Kolar, "Accurate Transient Calorimetric Measurement of Soft-Switching Losses of 10-kV SiC mosfets and Diodes," in IEEE Transactions on Power Electronics, vol. 33, no. 6, pp. 5240-5250, June 2018.

[7] J. A. Anderson, C. Gammeter, L. Schrittwieser and J. W. Kolar, "Accurate Calorimetric Switching Loss Measurement for 900 V 10 mΩ SiC mosfets," in IEEE Transactions on Power Electronics, vol. 32, no. 12, pp. 8963-8968, Dec. 2017.

[8] P. Papamanolis, T. Guillod, F. Krismer and J. W. Kolar, "Transient Calorimetric Measurement of Ferrite Core Losses up to 50 MHz," in IEEE Transactions on Power Electronics, vol. 36, no. 3, pp. 2548-2563, March 2021.

[9] L. Aarniovuori, A. Kosonen, P. Sillanpää and M. Niemelä, "High-Power Solar Inverter Efficiency Measurements by Calorimetric and Electric Methods," in IEEE Transactions on Power Electronics, vol. 28, no. 6, pp. 2798-2805, June 2013.

[10] D. Rothmund, T. Guillod, D. Bortis and J. W. Kolar, "99% Efficient 10 kV SiC-Based 7 kV/400 V DC Transformer for Future Data Centers," in IEEE Journal of Emerging and Selected Topics in Power Electronics, vol. 7, no. 2, pp. 753-767, June 2019.

[11] M. Guacci et al., "On the Origin of the C_{oss} -Losses in Soft-Switching GaN-on-Si Power HEMTs," in IEEE Journal of Emerging and Selected Topics in Power Electronics, vol. 7, no. 2, pp. 679-694, June 2019.

[12] M. Guacci et al., "Experimental Characterization of Silicon and Gallium Nitride 200 V Power Semiconductors for Modular/Multi-Level Converters Using Advanced Measurement Techniques," in IEEE Journal of Emerging and Selected Topics in Power Electronics, vol. 8, no. 3, pp. 2238-2254, Sept. 2020.

[13] D. Rothmund, T. Guillod, D. Bortis and J. W. Kolar, "99.1% Efficient 10 kV SiC-Based Medium-Voltage ZVS Bidirectional Single-Phase PFC AC/DC Stage," in IEEE Journal of Emerging and Selected Topics in Power Electronics, vol. 7, no. 2, pp. 779-797, June 2019.

[14] J. Rabkowski, D. Peftitsis and H. Nee, "Parallel-Operation of Discrete SiC BJTs in a 6-kW/250-kHz DC/DC Boost Converter," in IEEE Transactions on Power Electronics, vol. 29, no. 5, pp. 2482-2491, May 2014.

[15] Y. Wu, M. A. Shafi, A. M. Knight and R. A. McMahon, "Comparison of the Effects of Continuous and Discontinuous PWM Schemes on Power Losses of Voltage-Sourced Inverters for Induction Motor Drives," in IEEE Transactions on Power Electronics, vol. 26, no. 1, pp. 182-191, Jan. 2011.

[16] A. N. Hopkins, P. Proynov, N. McNeill, B. H. Stark and P. H. Mellor, "Achieving Efficiencies Exceeding 99% in a Super-Junction 5-kW DC–DC Converter Power Stage Through the Use of an Energy Recovery Snubber and Dead-Time Optimization," in IEEE Transactions on Power Electronics, vol. 33, no. 9, pp. 7510-7520, Sept. 2018.

[17] L. Hoffmann, C. Gautier, S. Lefebvre and F. Costa, "Optimization of the Driver of GaN Power Transistors Through Measurement of Their Thermal Behavior," in IEEE Transactions on Power Electronics, vol. 29, no. 5, pp. 2359-2366, May 2014.

[18] A. Jafari et al., "High-Accuracy Calibration-Free Calorimeter for the Measurement of Low Power Losses," in IEEE Transactions on Power Electronics, vol. 36, no. 1, pp. 23-28, Jan. 2021.